Ivet Elias,[1,2,3] Tura Ferré,[1,3] Laia Vilà,[1,2,3] Sergio Muñoz,[1,2,3] Alba Casellas,[1,3] Miquel Garcia,[1,2,3] Maria Molas,[1,2,3] Judith Agudo,[1,2,3] Carles Roca,[1,2,3] Jesús Ruberte,[1,3,4] Fatima Bosch,[1,2,3] and Sylvie Franckhauser[1,3]

ALOX5AP Overexpression in Adipose Tissue Leads to LXA_4 Production and Protection Against Diet-Induced Obesity and Insulin Resistance

Diabetes 2016;65:2139–2150 | DOI: 10.2337/db16-0040

Eicosanoids, such as leukotriene B4 (LTB_4) and lipoxin A4 (LXA_4), may play a key role during obesity. While LTB_4 is involved in adipose tissue inflammation and insulin resistance, LXA_4 may exert anti-inflammatory effects and alleviate hepatic steatosis. Both lipid mediators derive from the same pathway, in which arachidonate 5-lipoxygenase (ALOX5) and its partner, arachidonate 5-lipoxygenase–activating protein (ALOX5AP), are involved. ALOX5 and ALOX5AP expression is increased in humans and rodents with obesity and insulin resistance. We found that transgenic mice overexpressing ALOX5AP in adipose tissue had higher LXA_4 rather than higher LTB_4 levels, were leaner, and showed increased energy expenditure, partly due to browning of white adipose tissue (WAT). Upregulation of hepatic LXR and *Cyp7a1* led to higher bile acid synthesis, which may have contributed to increased thermogenesis. In addition, transgenic mice were protected against diet-induced obesity, insulin resistance, and inflammation. Finally, treatment of C57BL/6J mice with LXA_4, which showed browning of WAT, strongly suggests that LXA_4 is responsible for the transgenic mice phenotype. Thus, our data support that LXA_4 may hold great potential for the future development of therapeutic strategies for obesity and related diseases.

Obesity has emerged as one of the most important public health concerns of our society, with increasing incidence and morbidity. Obesity is associated with low-grade chronic inflammation of adipose tissue, which has been causally linked to the development of insulin resistance, type 2 diabetes, arthritis, cancer, cardiovascular diseases, asthma, and Alzheimer disease (1,2). In contrast to acute inflammation, in chronic inflammation the initiation phase is not followed by a resolution, and failure of resolution may be responsible for low-grade inflammation in obesity (3–5). During the unresolved inflammation, proinflammatory cytokines released by the adipose tissue act in a paracrine and systemic manner, promoting the development of insulin resistance in metabolic tissues (6,7). However, the mechanisms by which inflammation causes metabolic alterations have not been fully elucidated. The understanding of these processes is essential to the development of future treatments for obesity and type 2 diabetes, and both the prevention of adipose tissue inflammation and the promotion of its resolution may offer new therapeutic opportunities.

Lipid mediators, such as eicosanoids produced from arachidonic acid, play critical roles in inflammation and its resolution (5,6,8). Among them, leukotrienes are well-known proinflammatory molecules (9). These eicosanoids are derived from the enzymatic activity of arachidonate 5-lipoxygenase (ALOX5) and its partner, arachidonate 5-lipoxygenase–activating protein (ALOX5AP or FLAP). The activation of ALOX5/ALOX5AP is a crucial enzymatic step in the transformation of arachidonic acid into the unstable intermediate leukotriene A_4 (LTA_4), which is subsequently transformed into leukotriene B_4 (LTB_4) (5S, 12R-dihydroxy-eicosa-6Z, 8E, 10E, 14Z-tetraenoic acid). LTB_4, in addition to being a potent chemoattractant for leukocytes, enhances the release of proinflammatory adipokines, such as MCP-1 and interleukin (IL)-6, from obese

[1]Center of Animal Biotechnology and Gene Therapy, Universitat Autònoma de Barcelona, Barcelona, Spain
[2]Department of Biochemistry and Molecular Biology, School of Veterinary Medicine, Universitat Autònoma de Barcelona, Barcelona, Spain
[3]CIBER de Diabetes y Enfermedades Metabólicas Asociadas (CIBERDEM), Barcelona, Spain
[4]Department of Animal Health and Anatomy, School of Veterinary Medicine, Universitat Autònoma de Barcelona, Barcelona, Spain

Corresponding author: Sylvie Franckhauser, sylvie.franckhauser@uab.es.

Received 8 January 2016 and accepted 21 April 2016.

This article contains Supplementary Data online at http://diabetes.diabetesjournals.org/lookup/suppl/doi:10.2337/db16-0040/-/DC1.

adipose tissue (10,11). LTB_4 levels are elevated in adipose tissue during obesity (11–13), and LTB_4 has been described to play a role in the development of insulin resistance and to directly decrease insulin signaling in myocytes and hepatocytes in vitro (5,14,15). In addition, although the activation of the ALOX5/ALOX5AP complex is key to leukotriene synthesis, it can alternatively lead to the biosynthesis of other compounds, such as lipoxins (16). The intermediate LTA_4 can be converted to lipoxin A4 (LXA_4) (5S, 6R, 15S-trihydroxy-eicosa-7E, 9E, 11Z, 13E-tetraenoic acid) by action of 12-lipoxygenase (ALOX12) in humans (17,18) or in mice by arachidonate 15-lipoxygenase (ALOX15 or ALOX12/15) (19,20).

Lipoxins, which belong to the specialized proresolving mediator (SPM) family, exert anti-inflammatory effects and are involved in the resolution of inflammation (5). Treatment with LXA_4 of adipose tissue explants from aging mice—a model of adipose inflammation—leads to a decrease in IL-6 and restoration of GLUT4 and insulin receptor substrate (IRS)1 expression, indicating less inflammation and improved insulin sensitivity (21). In addition, it has recently been reported that treatment of mice with LXA_4 protects against high-fat diet (HFD)-induced adipose inflammation and hepatic lipid deposition without affecting glucose tolerance (22).

The key genes involved in LTB_4 and LXA_4 formation, *Alox5ap* and *Alox5,* are normally expressed in adipocytes and cells from the adipose stromal vascular fraction. Their expression is increased in adipose tissue of obese patients and animals with insulin resistance (11,12,23,24). Nevertheless, mice deficient for ALOX5 present an increase in body weight and body fat content and are more prone to fat accumulation when fed an HFD (13,25,26). In addition, other reports on the effects of the genetic disruption of *Alox5* on glucose homeostasis are contradictory (13,25,26). Thus, the role of ALOX5/ALOX5AP in the development of obesity and insulin resistance remains to be clearly established.

To address this issue, we generated transgenic mice overexpressing *Alox5ap* in adipose tissue. In these mice, ALOX5AP overexpression led to higher LXA_4 rather than higher LTB_4 levels. Transgenic mice were leaner and presented higher energy expenditure, in part due to browning of white adipose tissue (WAT), and were protected against diet-induced obesity and insulin resistance. Our results suggest that an increase in ALOX5/ALOX5AP activity has beneficial effects on metabolism, through an increase in circulating LXA_4, and protects against diet-induced obesity, insulin resistance, hepatic steatosis, and inflammation.

RESEARCH DESIGN AND METHODS

Animals

aP2/Alox5ap transgenic mice were generated by the Transgenic Animal Unit of the Center of Animal Biotechnology and Gene Therapy (CBATEG), Universitat Autònoma de Barcelona, by microinjection of a chimeric gene containing the entire coding sequence of the murine *Alox5ap* gene downstream of the 5.4 kb *aP2* promoter and upstream of the SV40 polyadenylation signal into fertilized oocytes from C57BL/6J × SJL mice. Microinjected embryos were then transferred into receptor CD1 females to obtain the *aP2/Alox5ap* transgenic mice. Mice were kept in a specific pathogen–free facility (Servei d'Estabulari de Ratolins–CBATEG) and maintained under a light-dark cycle of 12 h at 22°C. Mice were fed ad libitum with either a chow diet (Teklad Global 18% Protein Rodent Diet, 2018S; Envigo, Cambridgeshire, U.K.) or an HFD (Teklad Custom Diet, TD88137; Envigo) for 11 weeks. When stated, mice were fasted for 16 h. Experiments were carried out in wild-type and transgenic littermates between 4 and 6 months old. An indirect open-circuit calorimeter (Oxylet; Panlab, Cornellà, Spain) was used to monitor oxygen consumption and carbon dioxide production as previously described (27). Data were taken from the light and dark cycle. For LXA_4 stimulation, C57BL/6J male mice were given an intraperitoneal injection of 5 ng/g body wt LXA_4 (Merck Millipore, Billerica, MA) or vehicle 24 h and 48 h before sample collection. Animals were anesthetized and killed, and tissues of interest were excised and kept at −80°C or with formalin until analysis. Animal care and experimental procedures were approved by the Ethics Committee in Animal and Human Experimentation of the Universitat Autònoma de Barcelona.

Cell Culture

HepG2 cells were purchased from the European Collection of Cell Culture (Salisbury, U.K.) and cultured in minimum essential medium supplemented with 2 mmol/L glutamine, 1% nonessential amino acids, and 10% FCS (Gibco, Thermo Fisher Scientific, Grand Island, NY) at 37°C with 5% CO_2. HepG2 cells were later treated with 200 nmol/L LXA_4 or vehicle for 4 h.

Islet Isolation

Pancreata were perfused with 0.1 mg/mL collagenase I/II and thermolysin (Roche, Mannheim, Germany), digested for 19 min at 37°C, and purified from Histopaque 1077 gradient (Sigma-Aldrich, St. Louis, MO). Islets were handpicked under a stereomicroscope (Leica, Wetzlar, Germany) and used for RNA and protein extraction.

Gene Expression Analysis

Total RNA was extracted from different tissues using isolation reagent (TriPure, Roche, for nonfat tissues and QIAzol, Qiagen, Hilden, Germany, for fat tissues) and an Rneasy Mini kit (Qiagen). For Northern blot analysis, RNA samples were electrophoresed on a 1% agarose gel in MOPS buffer containing 2.2 mol/L formaldehyde. Membranes were hybridized with a ^{32}P-labeled *Alox5ap* cDNA probe obtained from PCR amplification using specific primers for *Alox5ap* cDNA (FW-5′AGCGTGGTCCAGAATGCG3′; RV-5′GATCCGCTTG CCGAAGATGTA3′) (GE Healthcare, Buckinghamshire, U.K.). For quantitative RT-PCR analysis, total RNA (1 μg) was retrotranscribed using the Transcriptor First Strand cDNA Synthesis kit (Roche). Quantitative PCR was

performed in a LightCycler (Roche) using the LightCycler 480 SyBr Green I Master Mix (Roche) and specific primers as described in Supplementary Table 2. Results were analyzed using the mathematical model of Pfaffl (28). All samples were processed in triplicate, and a mean Ct was calculated. The Ct for each transcript of interest was normalized by the Ct obtained for the reference gene *RplpO*.

Western Blot Analysis

Tissues were homogenized in protein lysis buffer. Western blot analysis was performed by standard procedures from total cellular homogenates of WAT, brown adipose tissue (BAT), liver, and islets as previously described (27). Briefly, tissues were homogenized in protein lysis buffer containing protease inhibitors. Protein expression was analyzed by electrophoresis of 15–30 μg different protein extracts in 10–12% SDS-PAGE gels transferred to polyvinylidene fluoride membranes and then incubated with Ponceau staining. Proteins were detected using 1:1,000 dilution of primary antibodies: rabbit polyclonal anti–uncoupling protein (UCP)1 (ab10983; Abcam, Cambridge, U.K.), rabbit polyclonal anti–5-lipoxygenase activating protein (FLAP) (bs-7556R; Bioss, Woburn, MA), rabbit polyclonal anti–liver X receptor (LXR)β (PA1-333; Thermo Fisher Scientific), and rabbit polyclonal anti–α-tubulin (ab4074; Abcam). Detection was performed using 1:10,000 dilution of horseradish peroxidase–labeled swine anti-rabbit immunoglobulins (P0217; Dako, Glostrup, Denmark) and Western blotting detection reagent (ECL Plus; Amersham, Freiburg, Germany).

Histological Analysis

Tissues were fixed for 24 h in formalin, embedded in paraffin, and sectioned. Sections were deparaffinized and stained with hematoxylin-eosin.

Glucose and Insulin Tolerance Tests

For the glucose tolerance test, awake mice, fasted overnight (16 h) with free access to water, were given an injection of 1 g glucose/kg body wt i.p., and glucose concentration was determined in blood samples at indicated time points using a Glucometer Elite analyzer (Bayer, Leverkusen, Germany). For the insulin tolerance test, 0.75 units of insulin/kg body wt i.p. (Humulin regular; Eli Lilly, Indianapolis, IN) was injected into awake fed mice, and glucose concentration was determined at indicated time points.

In Vivo Glucose-Stimulated Insulin Release

For insulin release determination, fasted mice were given an injection of 3 g glucose/kg body wt i.p. and venous blood was collected at indicated time points in chilled tubes and immediately centrifuged, and the plasma was stored at −20°C.

Ex Vivo LTB_4 and LXA_4 Release

Epididymal WAT (eWAT) and BAT explants from wild-type and transgenic mice were washed and incubated in 1 mL Krebs-Ringer bicarbonate HEPES buffer, pH 7.4, with either PD146176 (P4620; Sigma) or vehicle for 30 min, at 37°C at 300 rpm. LTB_4 and LXA_4 secretion in the media was then analyzed by ELISA.

Enzyme, Metabolite, and Hormone Assays

To determine pancreatic insulin content, whole pancreata were removed from the mice, weighted, and homogenized in 20 v/v of cold acidic ethanol (75% ethanol and 1.5% concentrated HCl) followed by 48 h of agitation at 4°C. Afterward, insulin was quantified in the supernatants of the samples diluted in phosphate buffer by radioimmunoassay (CIS Biointernational). Tissue triglyceride content was determined by extracting total lipids from liver samples with chloroform-methanol (2:1 v/v) as previously described (29). Triglycerides, total cholesterol, HDL cholesterol, and LDL cholesterol were quantified spectrophotometrically using an enzymatic assay kit (Horiba ABX, Montpellier, France). For determination of bile acid (BA) excretion rate, feces from individually housed mice were collected during a 24-h period and dried for 1 h at 70°C. The extraction was performed in 2 mL chloroform:methanol (2:1) following a method previously described (30). BAs from feces and from plasma were measured enzymatically (Randox Laboratory, Crumlin, U.K.). Serum nonesterified fatty acids (FFAs) were measured by the acyl-CoA synthase and acyl-CoA oxidase methods (Wako Chemicals GmbH, Neuss, Germany). All biochemical parameters were determined using a Pentra 400 Analyzer (Horiba-ABX). Glucose was determined using a Glucometer Elite analyzer (Bayer), and insulin levels were measured using the Rat Insulin ELISA kit (Crystal Chem, Chicago, IL). Leptin concentration was determined using the Mouse leptin ELISA kit (Crystal Chem). Serum MCP-1 levels were determined using the Mouse MCP-1 ELISA kit (eBioscience, San Diego, CA). Serum LTB_4 levels were measured with the LTB_4 ELISA kit (Enzo Life Sciences, Farmingdale, NY), and LXA_4 levels were measured in serum samples and in WAT extracts using the Mouse LXA_4 ELISA kit (CUSABIO BIOTECH Co. Ltd., Wuhan, China).

Statistical Analysis

All values are expressed as the mean ± SEM. Differences between groups were compared by Student *t* test. Statistical significance was considered if $P < 0.05$.

RESULTS

Adipose Tissue ALOX5AP Overexpression Leads to Increased Production of LXA_4 Rather Than LTB_4

For evaluation of the role of the *Alox5ap* gene in adipose tissue, transgenic mice overexpressing *Alox5ap* under the control of the *aP2* promoter were generated. The aP2 promoter has mostly been used to drive transgene expression in adipose tissue, although it has also been reported to allow expression in other tissues to a lesser extent (31–33). Two transgenic lines (Tg2 and Tg4) expressing high levels of *Alox5ap* mRNA in abdominal eWAT, measured either by Northern blot or by quantitative PCR (Fig. 1*A* and *B*), were analyzed. Since similar results have been obtained in both lines for a number of analyses, and to

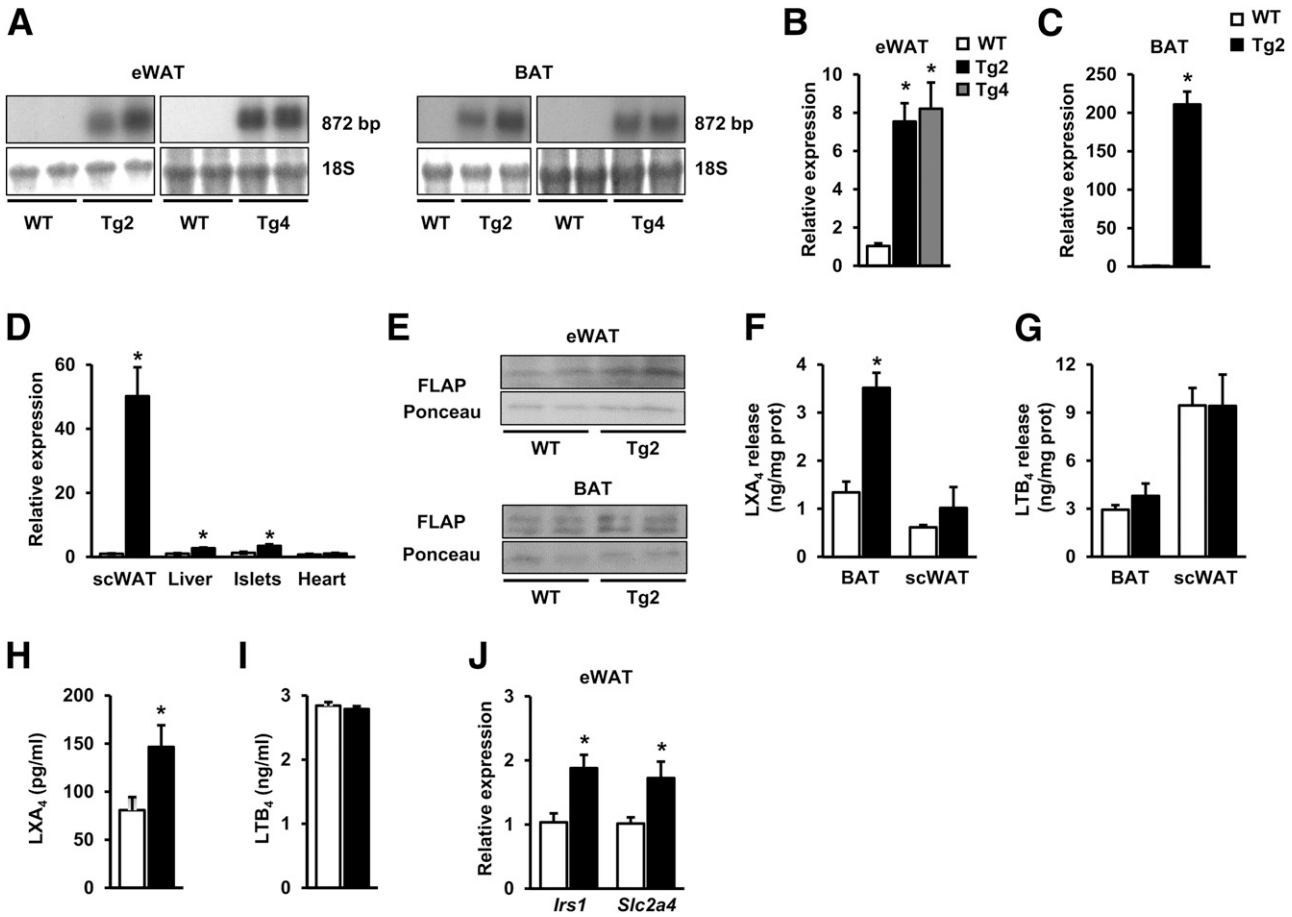

Figure 1— Increased production of LXA_4 rather than LTB_4 in ALOX5AP-overexpressing mice. *A*: Representative Northern blot of eWAT and BAT from wild-type (WT) and transgenic (Tg2 and Tg4) mice specific for *Alox5ap*. Methylene blue RNA staining of the membrane is shown as loading control. *B*: *Alox5ap* expression was analyzed by quantitative real-time PCR in eWAT (*B*), BAT (*C*), scWAT, liver, islets, and heart (*D*) from wild-type and Tg2 and Tg4 littermates (n = 5 animals/group). *E*: Representative Western blot analysis of ALOX5AP/FLAP expression in eWAT and BAT from wild-type and Tg2 mice showing a band of 16 kDa. Ponceau staining is shown as a loading control. *F* and *G*: LXA_4 (*F*) and LTB_4 (*G*) release was determined in BAT and scWAT explants from wild-type and Tg2 mice and measured by ELISA (n = 6 animals per group). *H* and *I*: Circulating LXA_4 (*H*) and LTB_4 (*I*) levels in wild-type and Tg2 mice were measured in serum samples by ELISA (n = 8 animals per group). *J*: *Irs1* and *Slc2a4* expression levels were analyzed by quantitative real-time PCR in eWAT from wild-type and Tg2 littermates (n = 5 animals per group). Data represent the mean ± SEM of at least 5 animals per group. *$P < 0.05$ vs. wild type. prot, protein.

avoid an unnecessary increase in the number of mice studied, Tg2 was randomly selected for a complete phenotyping. In Tg2 mice, expression was 200-fold increased in BAT and 50-fold higher in subcutaneous inguinal WAT (scWAT) (Fig. 1*C* and *D*). In nonadipose tissues such as liver or pancreatic islets, a slight increase in *Alox5ap* expression has also been observed, but to a lesser extent than in adipose tissue, while expression remained unchanged in heart (Fig. 1*D*). ALOX5AP/FLAP protein levels were also higher in eWAT and BAT from transgenic mice (Fig. 1*E*). Measurements of LXA_4 and LTB_4 production by adipose tissue explants showed that BAT from Tg2 released higher levels of LXA_4 but not LTB_4 compared with wild-type mice (Fig. 1*F* and *G*). A similar tendency was also observed in scWAT (Fig. 1*F* and *G*). Accordingly, circulating levels of LXA_4 were increased approximately twofold in Tg2 mice (Fig. 1*H*), while circulating LTB_4 levels were similar in both groups (Fig. 1*I*). In addition, specific inhibition of ALOX15 by PD146176 led to a reduction in LXA_4 production by BAT from Tg2 without affecting LTB_4 release (Supplementary Fig. 1*A*). This suggests that LXA_4 production in transgenic mice results from the sequential action of ALOX5 and ALOX15. However, expression of *Alox5* and *Alox15* remained significantly unchanged in scWAT and eWAT from Tg2 (Supplementary Fig. 1*B*). Moreover, adipose mRNA levels of *Irs1* and *Slc2a4* (GLUT4 gene), two genes whose expression increases after LXA_4 treatment (21), were higher in transgenic mice (Fig. 1*J*). Altogether, these results indicate that ALOX5AP overexpression leads to increased production of LXA_4 rather than LTB_4 in adipose tissue.

aP2/Alox5ap Transgenic Mice Are Leaner and Present Increased Energy Expenditure and Thermogenesis

Both lines of *aP2/Alox5ap* transgenic mice were smaller than wild-type mice, with a shorter naso-anal length and lower body weight (Fig. 2*A* and *B* and Supplementary Fig. 2*A* and *B*).

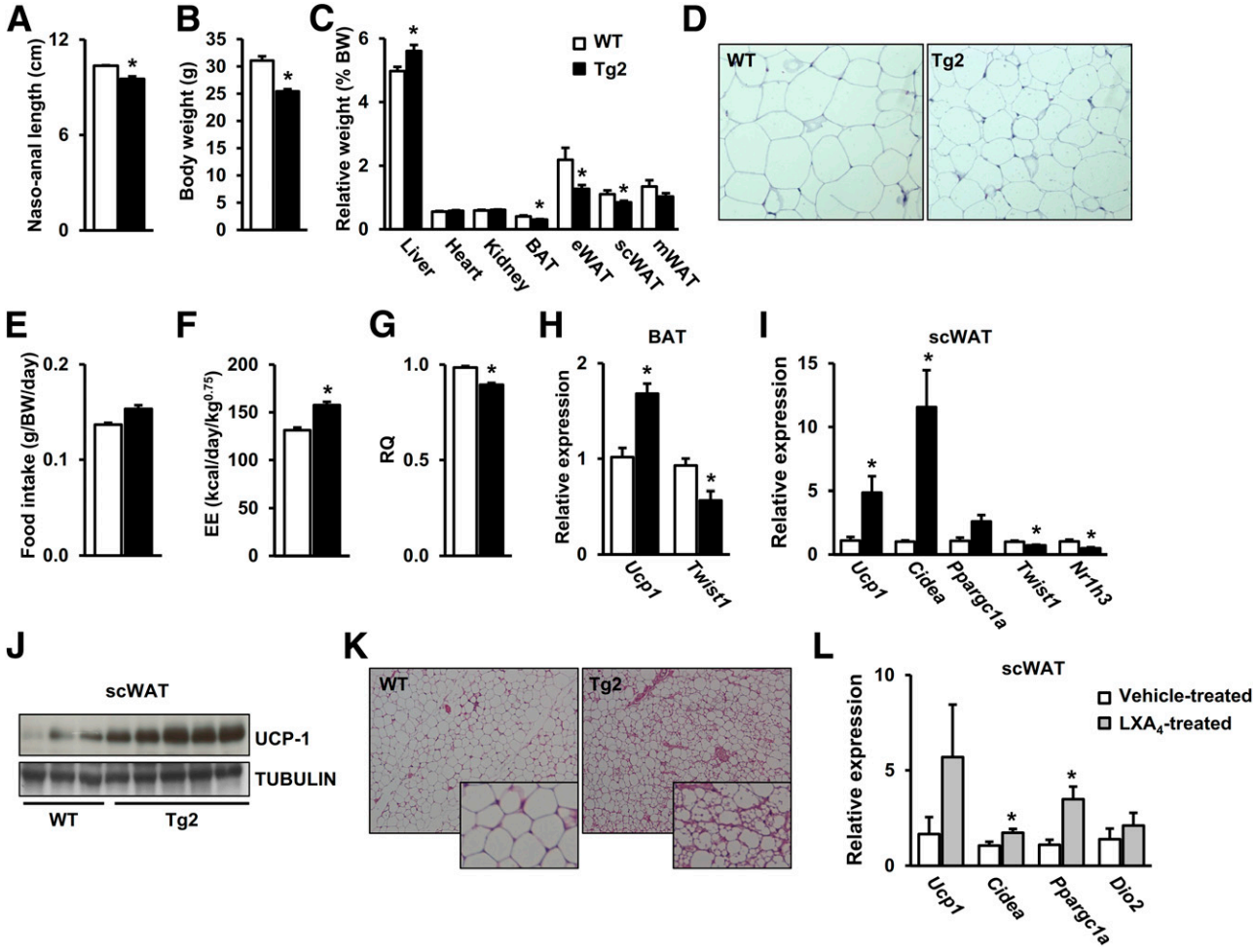

Figure 2—Reduced adiposity and enhanced thermogenesis in *Alox5ap* transgenic mice. *A* and *B*: Naso-anal length (*A*) and body weight (*B*) of wild-type (WT) and Tg2 mice were measured (n = 10 animals/group). See also Supplementary Fig. 1 for Tg4 line. *C*: Relative weight of different organs was calculated correcting each organ weight per total body weight. See also Supplementary Fig. 1 for Tg4 line. *D*: Representative sections of eWAT stained with hematoxylin-eosin (original magnification ×200). *E*: Food intake was measured and corrected per body weight (n = 10 animals/group). See also Supplementary Fig. 1 for Tg4 line. *F* and *G*: Energy expenditure (EE) (*F*) and RQ (*G*) were measured with an indirect open-circuit calorimeter in wild-type and Tg2 mice (n = 4 animals/group). See also Supplementary Fig. 1 for Tg4 line. *H* and *I*: Relative expression of BAT *Ucp1* and *Twist1* (*H*) and scWAT *Ucp1*, *Cidea*, *Ppargc1a*, *Twist1*, and *Nr1h3* (*I*) was analyzed by quantitative real-time PCR in wild-type and Tg2 mice (n = 5 animals/group). *J*: Representative Western blot analysis of UCP1 expression in scWAT showing a band of 32 kDa and using tubulin as a loading control. *K*: Representative sections of scWAT stained with hematoxylin-eosin (original magnification ×100). *L*: Relative expression of *Ucp1*, *Cidea*, *Ppargc1a*, and *Dio2* was analyzed by quantitative real-time PCR in scWAT of wild-type mice treated with 5 ng/g body wt LXA_4 or vehicle for 48 h (n = 6 animals/group). Data represent the mean ± SEM of at least 4 animals per group. *P < 0.05 vs. wild type. BW, body weight.

The weight of several main organs was also reduced (Supplementary Table 1). However, when corrected by total body weight, only the weight of BAT and WAT adipose depots was decreased in transgenic mice (Fig. 2*C* and Supplementary Fig. 2*C*). A smaller adipocyte size was also observed in the eWAT depot (Fig. 2*D*). This decrease in adiposity was not due to changes in food intake (Fig. 2*E* and Supplementary Fig. 2*D*) but, rather, to higher energy expenditure, as measured by indirect calorimetry (Fig. 2*F* and Supplementary Fig. 2*E*). In addition, the respiratory quotient (RQ) was reduced in transgenic mice, suggesting an increase in fat substrate oxidation (Fig. 2*G* and Supplementary Fig. 2*F*). Higher energy expenditure may reflect changes in thermogenesis. The mitochondrial UCP1 in BAT is essential to this function. BAT from transgenic mice expressed higher levels of *Ucp1* mRNA compared with wild-type mice and showed a decrease in the expression of *Twist1*, a negative regulator of *Ucp1* gene transcription (34) (Fig. 2*H*). Under certain conditions, adipocytes within scWAT have the capacity to express UCP1 and may contribute to thermogenesis (35,36). These adipocytes share characteristics with brown adipocytes, in particular, their multilocular lipid droplet morphology, their high mitochondrial content, and the expression of a set of markers such as *Ucp1*, *Cidea*, or *Ppargc1a* (36). In *aP2/Alox5ap* transgenic mice, enhanced expression of *Ucp1*, *Cidea*, and *Ppargc1a* mRNA was observed in scWAT (Fig. 2*I*). In addition, expression of two negative regulators of *Ucp1*, namely, *Twist1*

and *Nr1h3,* encoding for LXRα, was decreased (Fig. 2*I*). Higher UCP1 levels were also detected by Western blot in scWAT of transgenic mice (Fig. 2*J*). In addition, histological analysis of transgenic scWAT depots showed numerous clusters of multilocular adipocytes interspersed within the classical unilocular white adipocytes, indicating browning of scWAT (Fig. 2*K*). To determine whether LXA_4 is responsible for these effects, C57BL/6J mice were treated with LXA_4 for 48 h. Treated mice presented increased levels of *Ucp1* and browning markers in scWAT, such as *Cidea*, *Ppargc1*a, or *Dio2* (Fig. 2*L*). Thus, ALOX5AP overexpression, and the resulting increase in LXA_4, led to decreased adiposity, increased energy expenditure, and induction of browning of WAT.

aP2/Alox5ap Transgenic Mice Present Higher Levels of BAs in Circulation

Serum parameters reflecting lipid metabolism were examined. Circulating levels of triglycerides and FFAs remained unchanged in transgenic mice, whereas they presented higher levels of total cholesterol, reflecting an increase in HDL cholesterol without changes in LDL cholesterol (Fig. 3*A–E*).

In addition, circulating levels of BAs were higher in transgenic mice, as was the fecal BA excretion rate (Fig. 3*F* and *G*). The genes encoding for two enzymes involved in BA synthesis, namely, cholesterol 7α-hydroxylase (CYP7A1) and oxysterol 7α-hydroxylase (CYP7B1) (37–39), were upregulated in the liver of transgenic mice, and this may have led to higher plasma BA levels (Fig. 3*H*). The expression of LXR, a transcription factor key to the regulation of *Cyp7a1* expression (40), was examined next. Hepatic expression of both isoforms of LXR, LXRα (*Nr1h3* gene) and LXRβ (*Nr1h2* gene), was increased in transgenic animals (Fig. 3*I*), as were protein levels of LXRβ (Fig. 3*J* and *K*). A direct effect of LXA_4 on these genes has been further demonstrated in vitro. HepG2 cells treated with LXA_4 presented increased *CYP7A1* expression and a tendency to increase *NR1H2* expression compared with cells treated with vehicle (Fig. 3*L*). BAs have been shown to increase brown fat activity and energy expenditure through the G-protein–coupled BA receptor 1 (GPBAR1) (also called TGR5) and the activation of type 2 iodothyronine deionidase (DIO2) (41,42). In BAT from *aP2/Alox5ap* mice, *Gpbar1* expression levels were higher and *Dio2* expression showed a tendency to increase (Fig. 3*M*). These results suggest that overexpression of ALOX5AP in adipose tissue leads to upregulation of hepatic LXR, which in turn enhances *Cyp7a1* expression, thus increasing BA synthesis, contributing to higher thermogenesis and energy expenditure.

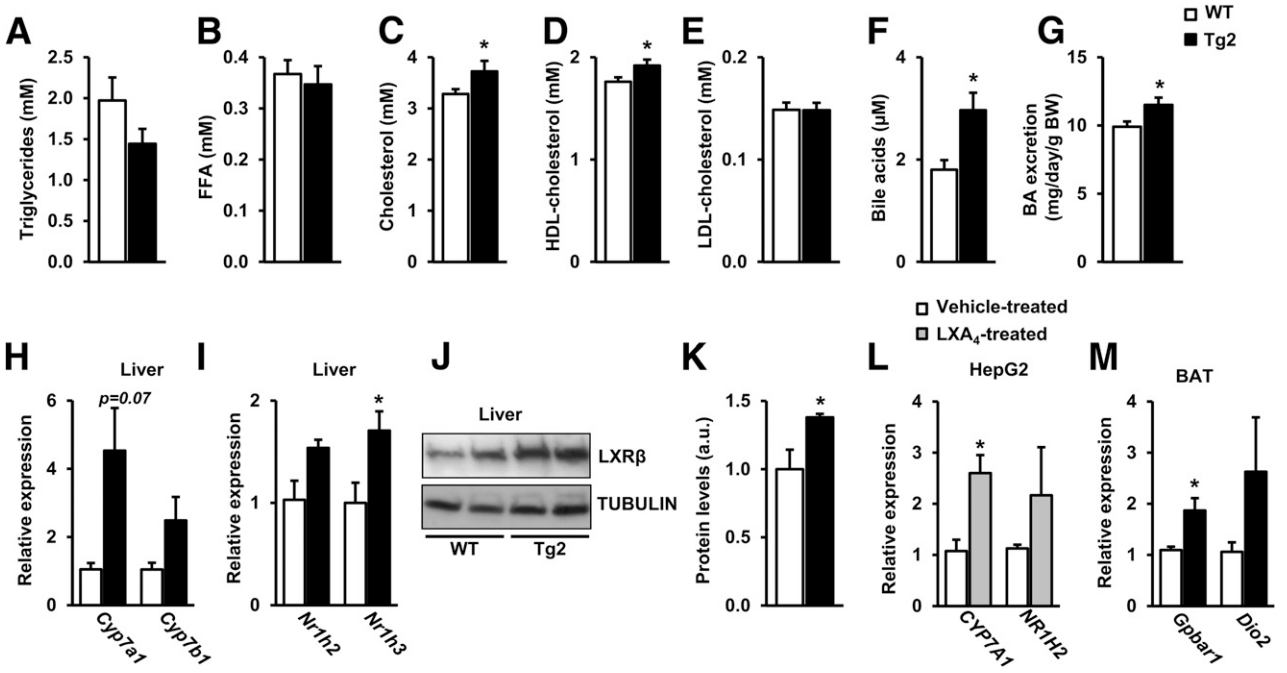

Figure 3—Transgenic mice present higher circulating BA levels. *A–F*: Levels of triglycerides (*A*), FFAs (*B*), total cholesterol (*C*), HDL cholesterol (*D*), LDL cholesterol (*E*), and BAs (*F*) were analyzed in serum of wild-type (WT) and Tg2 mice as indicated in RESEARCH DESIGN AND METHODS (n = 9 animals/group). *G*: BA excretion was determined in feces as indicated in RESEARCH DESIGN AND METHODS (n = 9 animals/group). *H*: Relative expression of liver *Cyp7a1* and *Cyp7b1* was analyzed by quantitative real-time PCR (n = 5 animals/group). *I*: Relative expression of liver *Nr1h2* and *Nr1h3* was analyzed by quantitative real-time PCR (n = 5 animals/group). *J*: Representative Western blot analysis of LXRβ expression in liver showing a band of 51 kDa corresponding to LXRβ and using tubulin as a loading control. *K*: Quantification of hepatic LXRβ expression normalized by tubulin content. *L*: Relative expression of *CYP7A1* and *NR1H2* was analyzed by quantitative real-time PCR in HepG2 cells treated with 200 nmol/L LXA_4 or vehicle for 4 h. (n = 6 wells/group.) *M*: Relative expression levels of BAT *Gpbar1* and *Dio2* were analyzed by quantitative real-time PCR (n = 5 animals/group). Data represent the mean ± SEM of at least 5 animals per group. *$P < 0.05$ vs. wild type. a.u., arbitrary units; BW, body weight.

Adipose Overexpression of ALOX5AP Leads to Impaired Insulin Secretion and Glucose Homeostasis

An intraperitoneal glucose tolerance test showed that transgenic mice displayed impaired glucose disposal after a glucose load (Fig. 4*A* and Supplementary Fig. 3*A*). Glucose intolerance may result from defects in insulin sensitivity and/or in inappropriate insulin secretion. When an insulin tolerance test was performed, transgenic mice showed an insulin response similar to that in wild-type mice, indicating preserved insulin sensitivity and suggesting a defect in insulin secretion (Fig. 4*B* and Supplementary Fig. 3*B*). Accordingly, circulating insulin levels showed a tendency to be lower (Fig. 4*C*) and the in vivo glucose-stimulated insulin release was altered in transgenic mice (Fig. 4*D* and Supplementary Fig. 3*C*). In particular, the first peak of insulin secretion was blunted (Fig. 4*D* and Supplementary Fig. 3*C*). In addition, pancreatic insulin content was increased, supporting the hypothesis that ALOX5AP overexpression led to a defect in insulin secretion without altering insulin synthesis (Fig. 4*E*). Since LXRβ may play a role in insulin secretion (43), its protein levels were examined in islets isolated from transgenic and wild-type mice. In islets from transgenic mice, LXRβ expression was 50% decreased, and this reduction may have contributed to the impairment of insulin secretion (Fig. 4*F* and *G*). Furthermore, in islets isolated from LXA_4-treated C57BL/6J mice, a tendency toward a decrease in LXRβ gene (*Nr1h2*) expression was also observed (Fig. 4*H*), suggesting a direct involvement of LXA_4.

Adipose Overexpression of ALOX5AP Prevents Diet-Induced Obesity and Insulin Resistance

The effects of ALOX5AP overexpression in adipose tissue were then examined under obesogenic conditions. In transgenic mice fed an HFD for 11 weeks, *Alox5ap* expression was increased in eWAT compared with wild-type mice, and LXA_4 circulating levels were also higher (Fig. 5*A* and *B*). In addition, whereas wild-type mice gained ~35% of their initial body weight, transgenic mice only gained 20% (Fig. 5*C*). Accordingly, the absolute and relative weights of epididymal white fat pad were lower in transgenic mice and adipocyte size was reduced (Fig. 5*D*–*F*). However, food intake was similar in both genotypes and the calculated food conversion efficiency was 50% lower in transgenic mice (Fig. 5*G* and *H*). This reduction may be partially explained by a tendency toward higher energy expenditure in transgenic mice (Fig. 5*I*), although no differences were observed in RQ between transgenic and wild-type mice (Fig. 5*J*). In addition, transgenic mice on an HFD showed high levels of UCP1 mRNA and protein in scWAT, indicating browning of WAT (Fig. 5*K* and *L*). In contrast, in BAT, *Ucp1* mRNA was not increased in

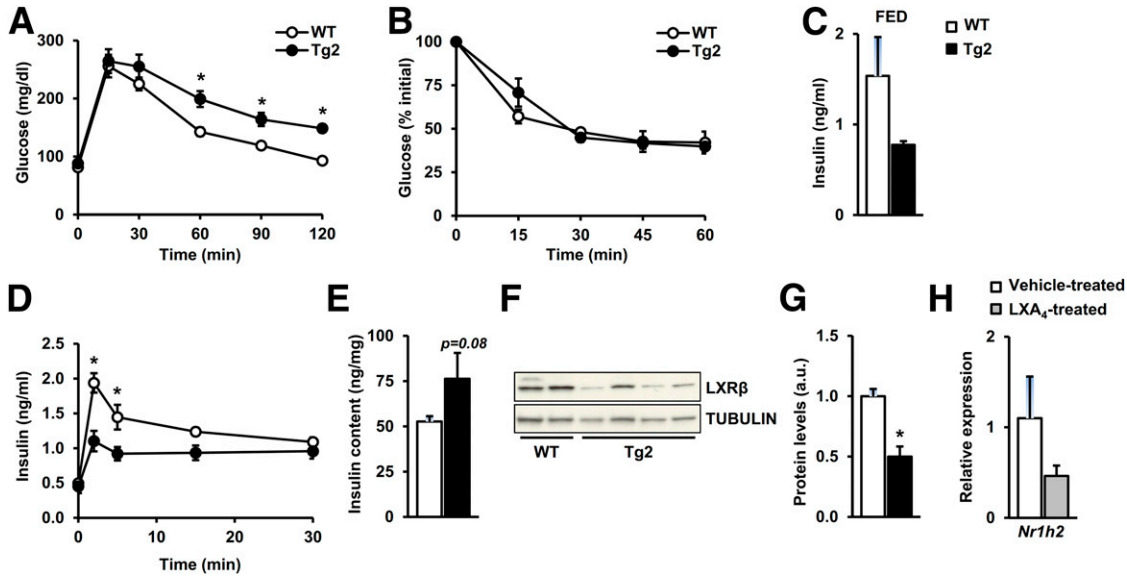

Figure 4—*Alox5ap* transgenic mice display altered insulin secretion and glucose homeostasis. *A*: Glucose tolerance was determined in starved wild-type (WT) and Tg2 mice (n = 8 animals/group) after an injection of 1 g glucose/kg body wt i.p., and blood glucose levels were measured at the indicated time points. See also Supplementary Fig. 2. *B*: Insulin sensitivity was determined in fed wild-type and Tg2 mice (n = 8 animals/group) after an injection of 0.75 units of insulin/kg body wt i.p. Results are calculated as percentage of initial blood glucose levels. See also Supplementary Fig. 2. *C*: Serum insulin levels were determined in fed conditions in wild-type and Tg2 mice (n = 8 animals/group). *D*: In vivo glucose-stimulated insulin release was determined in fasted wild-type and Tg2 mice (n = 7 animals/group) after a glucose load of 3 g/kg body wt at indicated time points. See also Supplementary Fig. 2. *E*: Whole-pancreas insulin content was measured as indicated in RESEARCH DESIGN AND METHODS. *F*: Representative Western blot analysis of LXRβ expression in islets showing a band of 51 kDa corresponding to LXRβ and using tubulin as a loading control. *G*: Quantification of islet LXRβ expression normalized by tubulin content. *H*: Relative expression of *Nr1h2* was analyzed by quantitative real-time PCR in islets of wild-type mice treated with 5 ng/g body wt LXA_4 or vehicle for 48 h (n = 6 animals/group). Data represent the mean ± SEM of at least 6 animals per group. *$P < 0.05$ vs. wild type. a.u., arbitrary units.

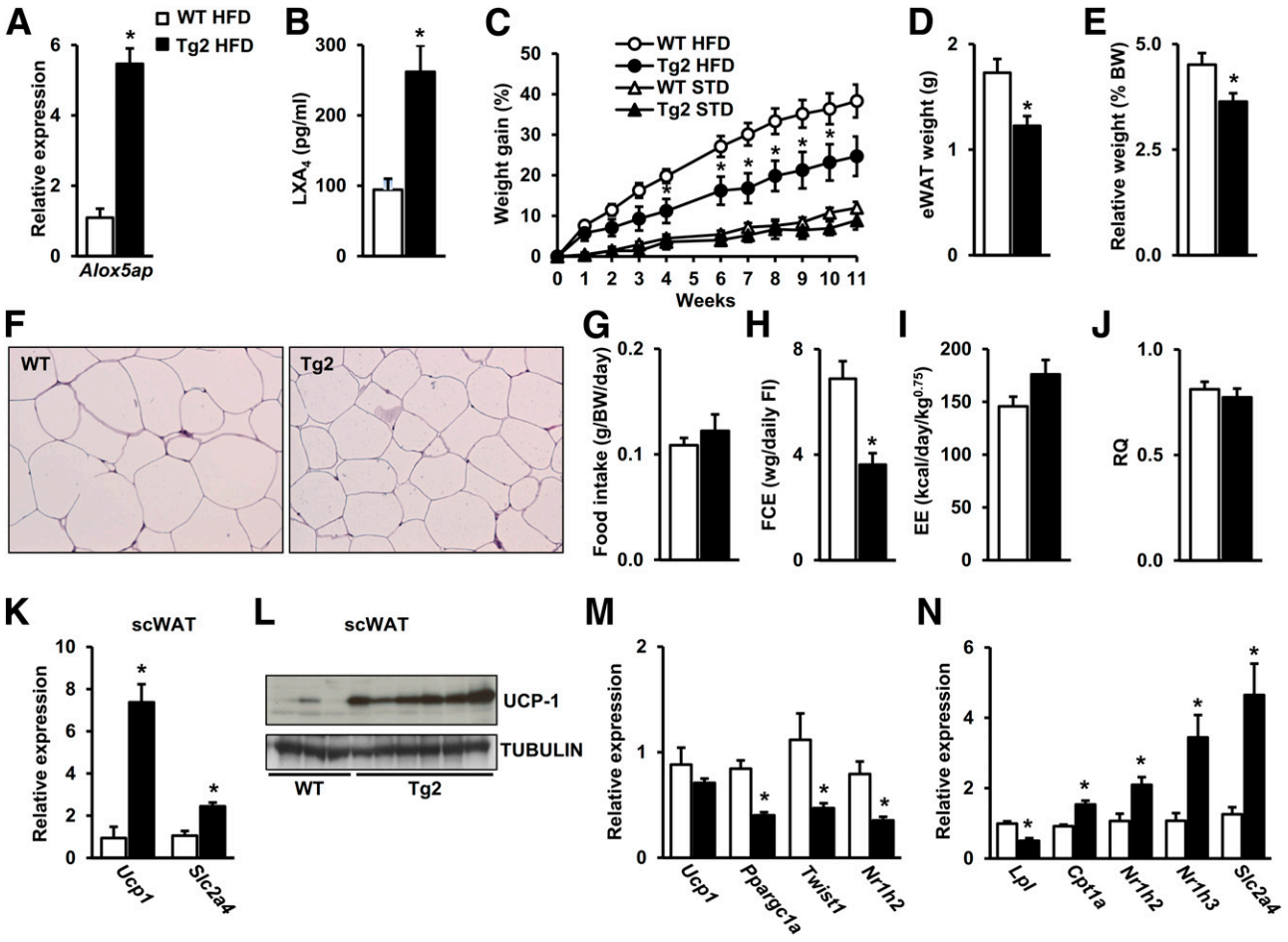

Figure 5—Adipose overexpression of *Alox5ap* prevents diet-induced obesity. *A*: Relative expression of eWAT *Alox5ap* was analyzed by quantitative real-time PCR in wild-type (WT) and Tg2 mice (n = 5 animals/group). *B*: LXA_4 serum levels in wild-type and Tg2 mice fed an HFD for 11 weeks (n = 8 animals/group). *C*: Weight gain in wild-type and Tg2 mice fed either a standard (STD) diet or an HFD for 11 weeks (n = 10 animals/group). *D* and *E*: eWAT weight (*D*) and relative eWAT weight (*E*) of wild-type and Tg2 mice fed an HFD for 11 weeks (n = 10 animals/group). *F*: Representative sections of eWAT stained with hematoxylin-eosin (original magnification ×200). *G* and *H*: Food intake (*G*) and food conversion efficiency (FCE) (*H*), calculated as weight gain (wg) per daily food intake (FI) (n = 10 animals/group). *I* and *J*: Energy expenditure (EE) (*I*) and RQ (*J*) measured with an indirect open-circuit calorimeter in wild-type and Tg2 mice fed an HFD (n = 4 animals/group). *K*: Relative expression levels of scWAT *Ucp1* and *Slc2a4* were analyzed by quantitative real-time PCR in wild-type and Tg2 mice (n = 5 animals/group). *L*: Representative Western blot analysis of UCP1 expression in scWAT showing a band of 32 kDa corresponding to UCP1. *M*: Relative expression of BAT *Ucp1*, *Ppargc1a*, *Twist1*, and *Nr1h2* was analyzed by quantitative real-time PCR in wild-type and Tg2 mice (n = 5 animals/group). *N*: Relative expression of eWAT *Lpl, Cpt1a, Nr1h2, Nr1h3*, and *Slc2a4* was analyzed by quantitative real-time PCR in wild-type and Tg2 mice (n = 5 animals/group). Data represent the mean ± SEM of at least 5 animals per group. *$P < 0.05$ vs. wild type fed an HFD. BW, body weight.

transgenic mice despite a decrease in the expression of *Twist1* and *Nr1h2* (Fig. 5*M*), both negative regulators of *Ucp1* expression. This may have been due to the observed decrease in *Ppargc1a* expression (Fig. 5*M*), which is critical for *Ucp1* transcription (34,44). Furthermore, the decrease in adipocyte size may also be caused by changes in WAT gene expression. In HFD-fed transgenic mice, the decrease in expression of lipoprotein lipase (*Lpl*), and the increase in *Cpt1a* expression (Fig. 5*N*), may have contributed to the smaller size of fat cells. In addition, enhanced expression of *Nr1h2* and *-3,* encoding, respectively, for LXR-β and -α, and previously described as possible regulators of lipolysis (45), may also have led to a decrease in WAT lipid deposition (Fig. 5*N*). In HFD-fed transgenic mice, *Slc2a4* expression was also upregulated, both in scWAT and eWAT (Fig. 5*K* and *N*). This may have resulted from the increased levels of LXRα and LXA_4 (21,46,47).

In addition, when challenged with a glucose load, transgenic mice fed an HFD presented an improvement in glucose tolerance with respect to wild-type mice, although they were more glucose intolerant than mice fed a standard diet (Fig. 6*A*). On an HFD, transgenic mice also showed better whole-body insulin sensitivity than wild-type mice (Fig. 6*B*). In agreement with the higher insulin sensitivity observed in transgenic mice fed an HFD, insulin levels were lower in these mice than in wild-type mice (Fig. 6*C*). In addition, the histological analysis of liver sections and the measurement of triglyceride content

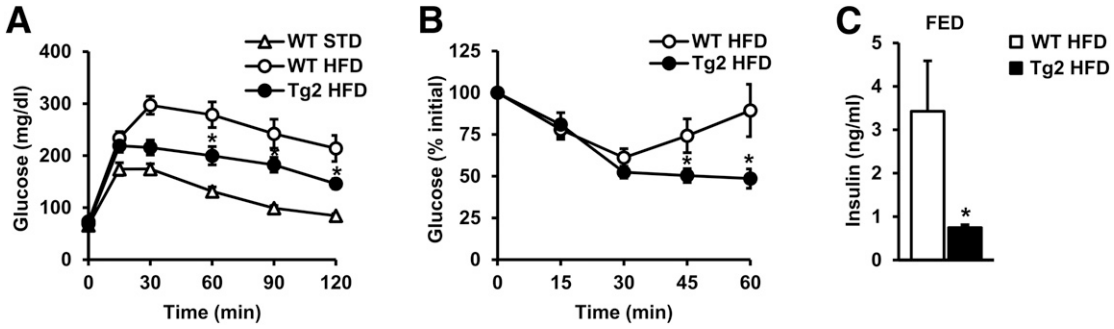

Figure 6—Adipose overexpression of ALOX5AP protects against diet-induced insulin resistance. *A*: Glucose tolerance was determined in starved wild-type (WT) and Tg2 mice (n = 10 animals/group) after an injection of 1 g glucose/kg body wt i.p., and blood glucose levels were measured at the indicated time points. *B*: Insulin sensitivity was determined in fed wild-type and Tg2 mice (n = 10 animals/group) after an injection of 0.75 units of insulin/kg body wt i.p. Results are calculated as percentage of initial blood glucose levels. *C*: Serum insulin levels in fed conditions (n = 10 animals/group). Data represent the mean ± SEM of at least 10 animals per group. *P < 0.05 vs. wild type fed an HFD. STD, standard diet.

showed fewer fat droplets in the liver of transgenic mice and decreased hepatic triglyceride content (Fig. 7*A* and *B*). In addition, transgenic mice showed hepatic downregulation of fatty acid synthase (*Fasn*) and *Lipin1* (Fig. 7*C*). Moreover, expression of sterol regulatory element–binding protein 1c (*Srebf1*) tended to decrease in transgenic mice, similar to *Nr1h3*, while *Nr1h2* expression was higher (Fig. 7*C*). Thus, adipose ALOX5AP overexpression prevents not only diet-induced weight gain but also hepatic steatosis and insulin resistance. In addition, transgenic mice on an HFD showed a tendency toward increased levels of BAs and upregulation of hepatic *Cyp7a1* and *Cyp7b1* (Fig. 7*D* and *E*). *Gpbar1* and *Dio2* expression levels were also increased in BAT from transgenic mice compared with wild-type mice (Fig. 7*F*). Since HFD-induced obesity is associated with adipose tissue inflammation, the eWAT mRNA levels of the macrophage marker F4/80 and the cytokine IL-6, both markers of inflammation, were examined next. Expression of both markers was reduced in transgenic mice, suggesting protection against diet-induced inflammation (Fig. 7*G*). In addition, circulating

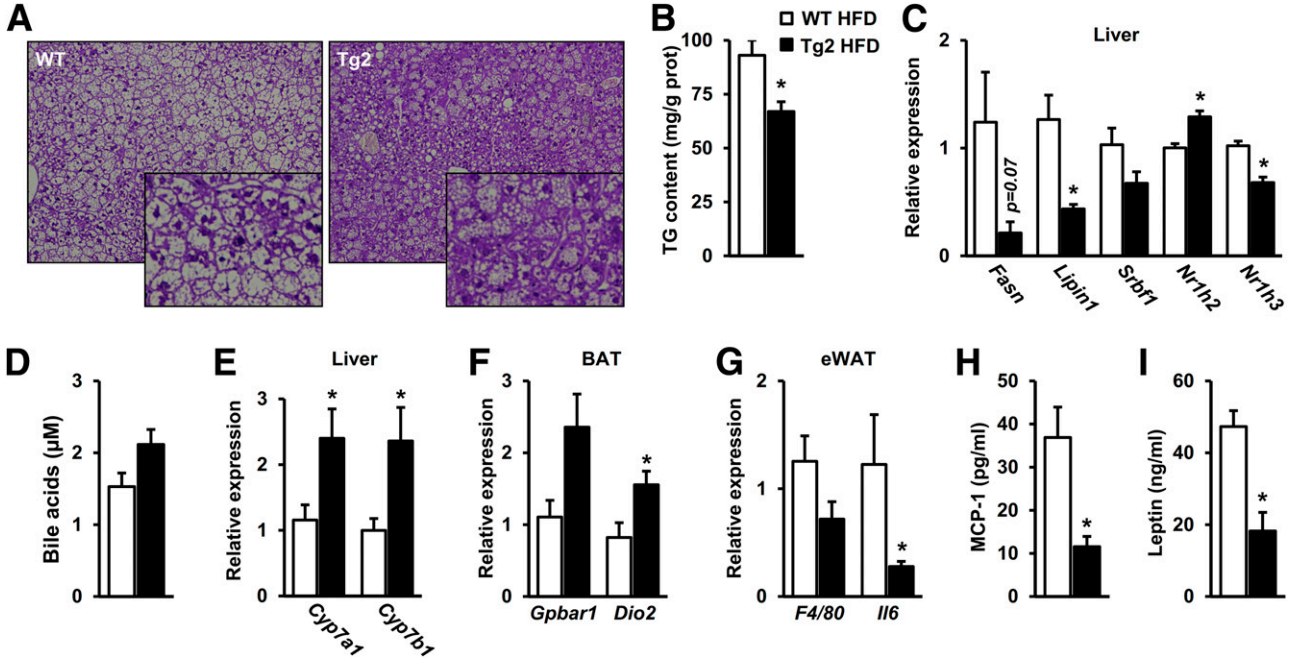

Figure 7—Adipose overexpression of ALOX5AP prevents diet-induced hepatic steatosis. *A*: Representative sections of liver stained with hematoxylin-eosin (original magnification ×100). *B*: Liver triglyceride (TG) content was determined as indicated in RESEARCH DESIGN AND METHODS (n = 10 animals/group). *C*: Relative expression of liver *Fasn, Lipin1, Srbf1, Nr1h2*, and *Nr1h3* was analyzed by quantitative real-time PCR. *D*: Serum BA levels in wild-type (WT) and Tg2 mice (n = 10 animals/group). *E–G*: Relative expression of liver *Cyp7a1* and *Cyp7b1* (*E*), BAT *Gpbar1* and *Dio2* (*F*), and eWAT *F4/80 and Il6* (*G*) was analyzed by quantitative real-time PCR. *H* and *I*: Serum levels of MCP-1 (*H*) and leptin (*I*) of wild-type and Tg2 mice (n = 10 animals/group) were analyzed as described in RESEARCH DESIGN AND METHODS. Data represent the mean ± SEM of at least 10 animals per group. *P < 0.05 vs. wild type fed an HFD. prot, protein.

MCP-1 and leptin levels were lower in transgenic mice fed an HFD than in wild-type mice (Fig. 7*H* and *I*). Altogether, these results suggest that overexpression of ALOX5AP prevents HFD-induced obesity, through browning of WAT, and protects against insulin resistance and inflammation.

DISCUSSION

Obesity has become a major public health problem in recent decades. Thus, finding new therapeutic approaches based on a better understanding of the pathophysiology of the disease is a key issue for our society. In this work, we demonstrate that overexpression of ALOX5AP leads to increased production of LXA_4 rather than LTB_4, decreased adiposity, and protection against HFD-induced obesity and insulin resistance.

The role of ALOX5/ALOX5AP in eicosanoid production has been recognized mainly for LTB_4 synthesis, although there is accumulating evidence that LXA_4, an SPM, is also a key product of this pathway (9,48,49). The mechanisms controlling the balance between LTB_4 and LXA_4 production are, however, as yet unclear. Surprisingly, in *aP2/Alox5ap* transgenic mice, ALOX5AP overexpression led to higher levels of LXA_4, whereas other reports have associated the increase in ALOX5/ALOX5AP in adipose tissue from rodent models of obesity with higher levels of LTB_4 (11,12,14,24). It has been reported that resolvin D1, another SPM, may increase LXA_4 and decrease LTB_4 production in macrophages (50). In addition, LXA_4 itself is able to decrease LTB_4 synthesis (50). Interestingly, obese adipose tissue displays lower resolvin D1 levels than lean tissue (51), and this may explain the increase in adipose tissue LTB_4 content observed in obesity.

The lean phenotype of ALOX5AP-overexpressing mice may at least partially be the result of an increase in energy expenditure as a consequence of the activation of thermogenesis in both BAT and scWAT. In agreement with this, ALOX5AP-overexpressing mice showed appearance of brown-like, multilocular adipocytes in scWAT, accompanied by upregulation of UCP1 expression and increased expression in markers of brown cells, indicating an enhancement of WAT browning. Furthermore, the resulting activation of thermogenesis may have also contributed to the improvement of insulin resistance observed in mice fed an HFD. In line with our results, the promotion of BAT activity or the browning of WAT has been reported to result in increased energy expenditure and protection against obesity and type 2 diabetes (35,36,52,53). These preclinical observations together with the recent discovery that browning of scWAT occurs in adult humans make this cell type an attractive therapeutic target for the treatment of obesity and type 2 diabetes (35,53,54). Our results suggest that molecules arising from the ALOX5/ALOX5AP pathway may have potential therapeutic effects. Here we demonstrate that one of these factors, LXA_4, is able to promote browning of scWAT in vivo. Moreover, other molecules, such as eicosapentanoic acid, a precursor of various factors belonging to the same family as LXA_4 (SPM family), are also able to induce the thermogenic capacity of subcutaneous adipocytes in vitro (55).

The observed effects of ALOX5AP overexpression on energy homeostasis may also rely on BA. Indeed, the increased levels of BAs in *Alox5ap* transgenic mice may have led to activation of BAT and higher energy expenditure. In this regard, it has been reported that BAs exert pleiotropic effects on metabolism, including activation of BAT leading to increased energy expenditure, which has prevented obesity and insulin resistance during HFD feeding (41). In humans, it has recently been reported that BAs activate BAT and increase energy expenditure (42). These effects of BA are mediated by the GPBAR1 (TGR5) receptor and dependent on the induction of DIO2 (42), expression of which was increased in BAT from *aP2/Alox5ap* transgenic mice. The observed increase in BA levels was probably due to hepatic *Cyp7a1* upregulation. Consistent with our findings, *Cyp7a1*-overexpressing transgenic mice presented higher BA synthesis; were protected against HFD-induced obesity, insulin resistance, and fatty liver; and presented higher levels of energy expenditure, associated with an increase in *Ucp1*, *Dio2*, and *Gpbar1* expression in BAT (56). In *aP2/Alox5ap* transgenic mice, upregulation of *Cyp7a1* was most likely due to an increase in hepatic LXR expression, a main regulator of *Cyp7a1* gene expression (40). Our results suggest that LXR mediates the effects of LXA_4 and plays a central role in the phenotype of *aP2/Alox5ap* mice. In particular, we show that LXA_4 induces *Nr1h2* expression in hepatoma cells and decreases it in islets. In agreement with this, it has been recently reported that LXA_4 controls LXRα expression and cholesterol metabolism in macrophages (57). Since LXR has raised much interest for the treatment of

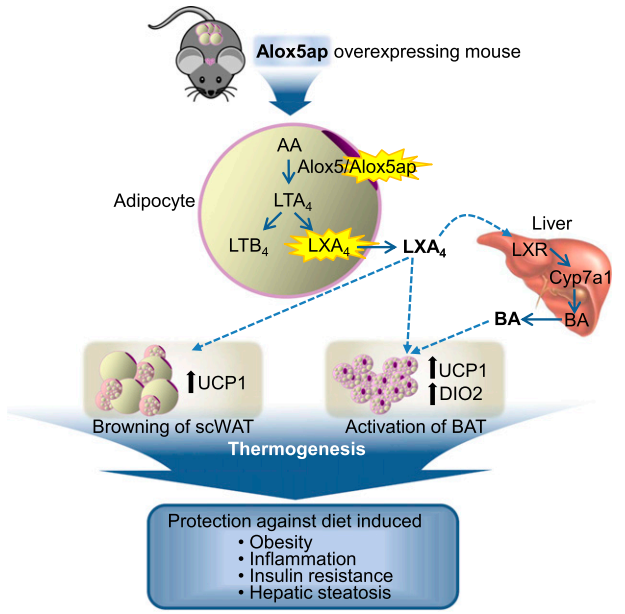

Figure 8—*Alox5ap* overexpression led to higher LXA_4 rather than LTB_4 levels and was associated with higher circulating BAs and energy expenditure, WAT browning, and protection against diet-induced obesity, inflammation, hepatic steatosis, and insulin resistance. AA, arachidonic acid.

atherosclerosis, diabetes, inflammation, Alzheimer disease, and cancer (58,59), a better understanding of its regulation by LXA_4 would be particularly relevant.

Despite the beneficial effects of ALOX5AP overexpression on energy metabolism, transgenic mice also presented glucose intolerance when fed a standard diet, probably due to a deficiency in insulin secretion. The observed decrease in LXRβ expression in islets may have contributed to this defect, as reported in mice deficient for LXRβ (43). LXRβ knockout mice were glucose intolerant due to impaired glucose-induced insulin secretion but displayed normal insulin sensitivity (43). Similarly, ALOX5AP-overexpressing mice presented alterations in glucose homeostasis but were not resistant to insulin and presented improved insulin sensitivity compared with wild-type mice when fed an HFD. This improvement may be, at least partially, due to the leaner phenotype of these mice, associated with decreased lipid accumulation in nonadipose tissues and decreased inflammation in WAT. The increase in *Cyp7b1* hepatic expression observed in transgenic mice may also have contributed to their protection against diet-induced glucose intolerance and hepatic steatosis, as suggested by the beneficial effects of hepatic *Cyp7b1* overexpression on these parameters previously reported (60).

In summary, our results clearly demonstrate that an increase in ALOX5AP expression may have beneficial effects on energy metabolism during obesity, increasing LXA_4 rather than LTB_4 levels and thus protecting against diet-induced obesity, through browning of WAT, and preventing insulin resistance, hepatic steatosis, and inflammation (Fig. 8). In agreement with our results, blocking LTA_4 hydrolase, the enzyme responsible for converting LTA_4 to LTB_4, leads to anti-inflammatory effects mediated by an increase in LXA_4 production (61,62). Our data also support the idea that LXA_4 deficiency plays a role in the development of obesity and its complications. In line with this, LXA_4 levels have been reported to be lower in adipose tissue of obese mice and to decrease with age (22,49). In addition, in humans, decreased LXA_4 levels accompanied by augmented levels of LTB_4 have been reported to be a hallmark of peri-wound fat from patients with a BMI >25 kg/m^2 (63).

Altogether, these results underscore the importance of acquiring a better understanding of the pathways involved in lipoxins and leukotrienes synthesis and their regulation, as they would be crucial for the development of new treatments for obesity and its comorbidities.

Acknowledgments. The authors thank Drs. Malcolm Watford (Rutgers University) and Virginia Haurigot (Universitat Autònoma de Barcelona) for helpful discussion; Mireia Zaguirre, Marta Moya, Jennifer Barrero, and Lidia Hernandez (Universitat Autònoma de Barcelona) for technical assistance; and Dr. Anna Pujol and Anna Arbós (Universitat Autònoma de Barcelona) for transgenic mice generation.

Funding. This work was supported by a grant from Ministerio de Economía y Competitividad of Spain, Instituto de Salud Carlos III (PI07/0313) to S.F. and from Ministerio de Economía y Competitividad, Plan Nacional I+D+I (SAF2014-54866-R), and Generalitat de Catalunya (Agència de Gestió d'Ajuts Universitaris i de Recerca, 2014-SGR1669, and Institució Catalana de Recerca i Estudis Avançats Academia) to F.B.

Duality of Interest. No potential conflicts of interest relevant to this article were reported.

Author Contributions. I.E. and S.F. designed the study, conducted the experiments, and wrote the manuscript. T.F., L.V., A.C., and M.G. conducted experiments and supported the work with key suggestions. S.M., M.M., J.A., C.R., and J.R. conducted experiments. F.B. designed the study, participated in discussion and editing, and secured funding. S.F. directed the project and secured funding. S.F. is the guarantor of this work and, as such, had full access to all the data in the study and takes responsibility for the integrity of the data and the accuracy of the data analysis.

References

1. Xu H, Barnes GT, Yang Q, et al. Chronic inflammation in fat plays a crucial role in the development of obesity-related insulin resistance. J Clin Invest 2003;112:1821–1830

2. Weisberg SP, McCann D, Desai M, Rosenbaum M, Leibel RL, Ferrante AW Jr. Obesity is associated with macrophage accumulation in adipose tissue. J Clin Invest 2003;112:1796–1808

3. Gilroy DW, Lawrence T, Perretti M, Rossi AG. Inflammatory resolution: new opportunities for drug discovery. Nat Rev Drug Discov 2004;3:401–416

4. Levy BD, Clish CB, Schmidt B, Gronert K, Serhan CN. Lipid mediator class switching during acute inflammation: signals in resolution. Nat Immunol 2001;2:612–619

5. Spite M, Clària J, Serhan CN. Resolvins, specialized proresolving lipid mediators, and their potential roles in metabolic diseases. Cell Metab 2014;19:21–36

6. Masoodi M, Kuda O, Rossmeisl M, Flachs P, Kopecky J. Lipid signaling in adipose tissue: connecting inflammation & metabolism. Biochim Biophys Acta 2015;1851:503–518

7. Hotamisligil GS, Shargill NS, Spiegelman BM. Adipose expression of tumor necrosis factor-alpha: direct role in obesity-linked insulin resistance. Science 1993;259:87–91

8. Dennis EA, Norris PC. Eicosanoid storm in infection and inflammation. Nat Rev Immunol 2015;15:511–523

9. Rådmark O, Werz O, Steinhilber D, Samuelsson B. 5-lipoxygenase, a key enzyme for leukotriene biosynthesis in health and disease. Biochim Biophys Acta 2015;1851:331–339

10. Filgueiras LR, Serezani CH, Jancar S. Leukotriene B4 as a potential therapeutic target for the treatment of metabolic disorders. Front Immunol 2015;6:515

11. Horrillo R, González-Périz A, Martínez-Clemente M, et al. 5-lipoxygenase activating protein signals adipose tissue inflammation and lipid dysfunction in experimental obesity. J Immunol 2010;184:3978–3987

12. Chakrabarti SK, Wen Y, Dobrian AD, et al. Evidence for activation of inflammatory lipoxygenase pathways in visceral adipose tissue of obese Zucker rats. Am J Physiol Endocrinol Metab 2011;300:E175–E187

13. Mothe-Satney I, Filloux C, Amghar H, et al. Adipocytes secrete leukotrienes: contribution to obesity-associated inflammation and insulin resistance in mice. Diabetes 2012;61:2311–2319

14. Li P, Oh Y, Bandyopadhyay G, et al. LTB4 promotes insulin resistance in obese mice by acting on macrophages, hepatocytes and myocytes. Nat Med 2015;21:239–247

15. Spite M, Hellmann J, Tang Y, et al. Deficiency of the leukotriene B4 receptor, BLT-1, protects against systemic insulin resistance in diet-induced obesity. J Immunol 2011;187:1942–1949

16. Sala A, Folco G, Murphy RC. Transcellular biosynthesis of eicosanoids. Pharmacol Rep 2010;62:503–510

17. Serhan CN, Sheppard KA. Lipoxin formation during human neutrophil-platelet interactions. Evidence for the transformation of leukotriene A4 by platelet 12-lipoxygenase in vitro. J Clin Invest 1990;85:772–780

18. Edenius C, Haeggström J, Lindgren JA. Transcellular conversion of endogenous arachidonic acid to lipoxins in mixed human platelet-granulocyte suspensions. Biochem Biophys Res Commun 1988;157:801–807

19. Merched AJ, Ko K, Gotlinger KH, Serhan CN, Chan L. Atherosclerosis: evidence for impairment of resolution of vascular inflammation governed by specific lipid mediators. FASEB J 2008;22:3595–3606

20. Krönke G, Katzenbeisser J, Uderhardt S, et al. 12/15-lipoxygenase counteracts inflammation and tissue damage in arthritis. J Immunol 2009;183:3383–3389
21. Börgeson E, McGillicuddy FC, Harford KA, et al. Lipoxin A4 attenuates adipose inflammation. FASEB J 2012;26:4287–4294
22. Börgeson E, Johnson AM, Lee YS, et al. Lipoxin A4 attenuates obesity-induced adipose inflammation and associated liver and kidney disease. Cell Metab 2015;22:125–137
23. Kaaman M, Rydén M, Axelsson T, et al. ALOX5AP expression, but not gene haplotypes, is associated with obesity and insulin resistance. Int J Obes 2006;30:447–452
24. Bäck M, Sultan A, Ovchinnikova O, Hansson GK. 5-lipoxygenase-activating protein: a potential link between innate and adaptive immunity in atherosclerosis and adipose tissue inflammation. Circ Res 2007;100:946–949
25. Mehrabian M, Schulthess FT, Nebohacova M, et al. Identification of ALOX5 as a gene regulating adiposity and pancreatic function. Diabetologia 2008;51:978–988
26. Martínez-Clemente M, Ferré N, González-Périz A, et al. 5-lipoxygenase deficiency reduces hepatic inflammation and tumor necrosis factor alpha-induced hepatocyte damage in hyperlipidemia-prone ApoE-null mice. Hepatology 2010;51:817–827
27. Franckhauser S, Muñoz S, Elias I, Ferre T, Bosch F. Adipose overexpression of phosphoenolpyruvate carboxykinase leads to high susceptibility to diet-induced insulin resistance and obesity. Diabetes 2006;55:273–280
28. Pfaffl MW. A new mathematical model for relative quantification in real-time RT-PCR. Nucleic Acids Res 2001;29:e45
29. Carr TP, Andresen CJ, Rudel LL. Enzymatic determination of triglyceride, free cholesterol, and total cholesterol in tissue lipid extracts. Clin Biochem 1993;26:39–42
30. Mataki C, Magnier BC, Houten SM, et al. Compromised intestinal lipid absorption in mice with a liver-specific deficiency of liver receptor homolog 1. Mol Cell Biol 2007;27:8330–8339
31. Graves RA, Tontonoz P, Platt KA, Ross SR, Spiegelman BM. Identification of a fat cell enhancer: analysis of requirements for adipose tissue-specific gene expression. J Cell Biochem 1992;49:219–224
32. Lee KY, Russell SJ, Ussar S, et al. Lessons on conditional gene targeting in mouse adipose tissue. Diabetes 2013;62:864–874
33. Mullican SE, Tomaru T, Gaddis CA, Peed LC, Sundaram A, Lazar MA. A novel adipose-specific gene deletion model demonstrates potential pitfalls of existing methods. Mol Endocrinol 2013;27:127–134
34. Pan D, Fujimoto M, Lopes A, Wang YX. Twist-1 is a PPARdelta-inducible, negative-feedback regulator of PGC-1alpha in brown fat metabolism. Cell 2009;137:73–86
35. Poher AL, Altirriba J, Veyrat-Durebex C, Rohner-Jeanrenaud F. Brown adipose tissue activity as a target for the treatment of obesity/insulin resistance. Front Physiol 2015;6:4
36. Harms M, Seale P. Brown and beige fat: development, function and therapeutic potential. Nat Med 2013;19:1252–1263
37. Schwarz M, Lund EG, Setchell KD, et al. Disruption of cholesterol 7alpha-hydroxylase gene in mice. II. Bile acid deficiency is overcome by induction of oxysterol 7alpha-hydroxylase. J Biol Chem 1996;271:18024–18031
38. Schwarz M, Russell DW, Dietschy JM, Turley SD. Alternate pathways of bile acid synthesis in the cholesterol 7alpha-hydroxylase knockout mouse are not upregulated by either cholesterol or cholestyramine feeding. J Lipid Res 2001;42:1594–1603
39. de Aguiar Vallim TQ, Tarling EJ, Edwards PA. Pleiotropic roles of bile acids in metabolism. Cell Metab 2013;17:657–669
40. Lehmann JM, Kliewer SA, Moore LB, et al. Activation of the nuclear receptor LXR by oxysterols defines a new hormone response pathway. J Biol Chem 1997;272:3137–3140
41. Watanabe M, Houten SM, Mataki C, et al. Bile acids induce energy expenditure by promoting intracellular thyroid hormone activation. Nature 2006;439:484–489
42. Broeders EP, Nascimento EB, Havekes B, et al. The bile acid chenodeoxycholic acid increases human brown adipose tissue activity. Cell Metab 2015;22:418–426
43. Gerin I, Dolinsky VW, Shackman JG, et al. LXRbeta is required for adipocyte growth, glucose homeostasis, and beta cell function. J Biol Chem 2005;280:23024–23031
44. Lin J, Handschin C, Spiegelman BM. Metabolic control through the PGC-1 family of transcription coactivators. Cell Metab 2005;1:361–370
45. Laurencikiene J, Rydén M. Liver X receptors and fat cell metabolism. Int J Obes 2012;36:1494–1502
46. Dalen KT, Ulven SM, Bamberg K, Gustafsson JA, Nebb HI. Expression of the insulin-responsive glucose transporter GLUT4 in adipocytes is dependent on liver X receptor alpha. J Biol Chem 2003;278:48283–48291
47. Ross SE, Erickson RL, Gerin I, et al. Microarray analyses during adipogenesis: understanding the effects of Wnt signaling on adipogenesis and the roles of liver X receptor alpha in adipocyte metabolism. Mol Cell Biol 2002;22:5989–5999
48. Shryock N, McBerry C, Salazar Gonzalez RM, Janes S, Costa FT, Aliberti J. Lipoxin A_4 and 15-epi-lipoxin A_4 protect against experimental cerebral malaria by inhibiting IL-12/IFN-γ in the brain. PLoS One 2013;8:e61882
49. Leo LM, Almeida-Corrêa S, Canetti CA, Amaral OB, Bozza FA, Pamplona FA. Age-dependent relevance of endogenous 5-lipoxygenase derivatives in anxiety-like behavior in mice. PLoS One 2014;9:e85009
50. Fredman G, Ozcan L, Spolitu S, et al. Resolvin D1 limits 5-lipoxygenase nuclear localization and leukotriene B4 synthesis by inhibiting a calcium-activated kinase pathway. Proc Natl Acad Sci U S A 2014;111:14530–14535
51. Clària J, Dalli J, Yacoubian S, Gao F, Serhan CN. Resolvin D1 and resolvin D2 govern local inflammatory tone in obese fat. J Immunol 2012;189:2597–2605
52. Seale P, Conroe HM, Estall J, et al. Prdm16 determines the thermogenic program of subcutaneous white adipose tissue in mice. J Clin Invest 2011;121:96–105
53. Peirce V, Vidal-Puig A. Regulation of glucose homoeostasis by brown adipose tissue. Lancet Diabetes Endocrinol 2013;1:353–360
54. Sidossis LS, Porter C, Saraf MK, et al. Browning of subcutaneous white adipose tissue in humans after severe adrenergic stress. Cell Metab 2015;22:219–227
55. Zhao M, Chen X. Eicosapentaenoic acid promotes thermogenic and fatty acid storage capacity in mouse subcutaneous adipocytes. Biochem Biophys Res Commun 2014;450:1446–1451
56. Li T, Owsley E, Matozel M, Hsu P, Novak CM, Chiang JY. Transgenic expression of cholesterol 7alpha-hydroxylase in the liver prevents high-fat diet-induced obesity and insulin resistance in mice. Hepatology 2010;52:678–690
57. Sha YH, Hu YW, Gao JJ, et al. Lipoxin A4 promotes ABCA1 expression and cholesterol efflux through the LXRα signaling pathway in THP-1 macrophage-derived foam cells. Int J Clin Exp Pathol 2015;8:6708–6715
58. Hong C, Tontonoz P. Liver X receptors in lipid metabolism: opportunities for drug discovery. Nat Rev Drug Discov 2014;13:433–444
59. Loren J, Huang Z, Laffitte BA, Molteni V. Liver X receptor modulators: a review of recently patented compounds (2009 - 2012). Expert Opin Ther Pat 2013;23:1317–1335
60. Fu S, Fan J, Blanco J, et al. Polysome profiling in liver identifies dynamic regulation of endoplasmic reticulum translatome by obesity and fasting. PLoS Genet 2012;8:e1002902
61. Rao NL, Dunford PJ, Xue X, et al. Anti-inflammatory activity of a potent, selective leukotriene A4 hydrolase inhibitor in comparison with the 5-lipoxygenase inhibitor zileuton. J Pharmacol Exp Ther 2007;321:1154–1160
62. Rao NL, Riley JP, Banie H, et al. Leukotriene A(4) hydrolase inhibition attenuates allergic airway inflammation and hyperresponsiveness. Am J Respir Crit Care Med 2010;181:899–907
63. Clària J, Nguyen BT, Madenci AL, Ozaki CK, Serhan CN. Diversity of lipid mediators in human adipose tissue depots. Am J Physiol Cell Physiol 2013;304:C1141–C1149